Dielectric response of a polarizable system with quenched disorder

Xueyu Song[1,2] and David Chandler[1]
[1]*Department of Chemistry, University of California, Berkeley, California 94720*
[2]*Department of Chemistry, Iowa State University, Ames, Iowa 50011*
(Received 4 May 2000)

We present and analyze a lattice model of a disordered dielectric material. In the model, the local polarizability is a quenched statistical variable. Using a reaction field approach, the dielectric response of the model can be cast in terms of an effective Hamiltonian for a finite primary system coupled to its effective average medium determined self-consistently. A real space renormalization group analysis is carried out by recursively increasing the size of the primary system. The analysis determines the length scale dependence of the local polarizability distribution. For the case of isotropic disorder considered in this paper, we show that the width of the distribution decays algebraically with increasing lattice spacing. We also compute the distribution of solvation and reorganization energies pertinent to kinetics of electron transfer.

PACS number(s): 61.20.Gy, 77.22.Gm

I. INTRODUCTION

Polarization fluctuations play a dominant role in thermal electron transfer, energy transfer and solvation dynamics. Substantial theoretical, computational and experimental efforts have been devoted to understand these fluctuations and the associated dielectric responses. These efforts have established a few simple and useful facts. One of the most important is that for polar liquids, the dielectric response to a solute charge distribution change is essentially a linear response [1,2]. Another is that both the static and dynamical consequences of this linear response are well-approximated by dielectric continuum theory [3–6]. One might ask if there are implications drawn from these facts that apply to disordered systems that are not entirely liquid. For example, what aspects of dielectric continuum theory can be used when considering the dielectric response of a glass, a protein, or a zeolite? This paper provides a formalism with which this question can be answered, and with which the behaviors of these disordered or inhomogeneous systems can be modeled.

We employ quenched statistical distributions to describe inhomogeneities and disorder. As such, our strategy takes a middle ground between dielectric continuum theory and explicit atomistic modeling. The pictures we draw are therefore impressionistic caricatures of reality. For example, a particular protein environment contains specific regions of high polarity (aqueous and hydrophilic) and specific regions of low polarity (nonpolar and hydrophobic). In the statistical view we adopt, we imagine predicting the dielectric behavior of that environment as if it is a representative member of an ensemble of environments. The ensemble is characterized by probabilities for where polar or nonpolar patches are located. For example, if we are interested in the ultrafast solvation dynamics in a protein environment the slow conformational motion of the protein will create such an ensemble.

In general, these distributions could be very complicated. For this paper, however, we confine our attention to the simplest of such distributions, one that is bimodal, isotropic, and uncorrelated. As described in Sec. II, we consider a dielectric system partitioned on a uniform grid, with grid lines separated by a distance a, forming a cubic lattice. Each lattice cell has volume a^3, and a local polarizability that can take on either one of two possible values (such as a larger polarizability of the high polarity region of a protein and lower polarizability of the nonpolar region of the protein). The dielectric behavior of this system is the same as that predicted by dielectric continuum theory when the polarizabilities are constant over the whole lattice [8–11]. Further, when coarse-grained over large enough length scales, we expect that deviations from some kind of mean polarizability are negligible in this model. Thus, its macroscopic dielectric behavior is that of dielectric continuum theory. On length scales of a or small multiples of a, however, we will see that its behavior differs significantly from this macroscopic limit.

We analyze the differences between the microscopic and macroscopic regimes through a renormalization group calculation. The essential feature of this calculation, detailed in Sec. III, is a length scale renormalization of the local polarizability distribution. Such spatial renormalization group calculations have been used in other quenched disordered models with short-ranged interactions [12]. The renormalization equations are derived by employing a reaction field description of the coupling of a finite primary system with an effective average medium determined self-consistently. On the microscopic length scale a, the distribution of local polarizability is simply bimodal, by construction. But as the length scale grows, the distribution approaches a narrow Gaussian, with width that vanishes as an inverse power of the length scale. The macroscopic limit corresponds to the limit in which the distribution has zero width.

We use the same type of analysis in Sec. IV to study the distribution of solvation and reorganization energies for a dipolar particle of a given size solvated by this model dielectric medium. It is found that the reorganization energy is distributed over a range of values and different microenvironments of the dipolar particle contribute to the width of such a distribution.

The specific results we establish for this isotropically disordered model are of some interest. For example, the predicted distribution of reorganization energies implies a specific and, in principle, measurable nonexponential kinetics for electron transfer occurring in real systems that approximates the model. More significant, however, is the methodology we establish in this paper. Others before us have con-

 ©2000 The American Physical Society

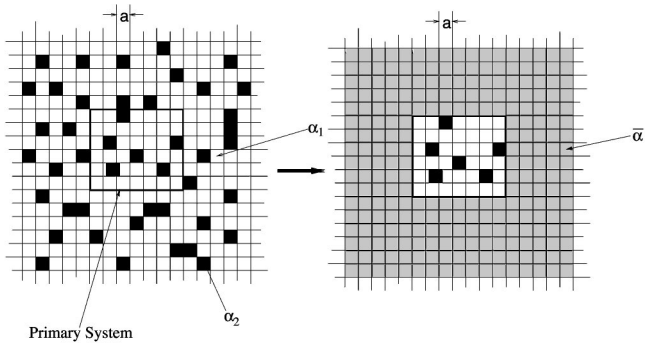

FIG. 1. Schematic illustration of a realization of the disordered dielectric (left) and the reduced effective system (right). The primary system is marked by a bold cube. The black cells represent dipoles with higher polarizability and the white cells represent dipoles with lower polarizability. The secondary system cell polarizability ($\bar{\alpha}$, the gray cells) is determined self-consistently as described in the text.

sidered dielectric properties of a model with disorder, employing an effective medium approximation [13] or simulation [14]. A reaction field calculation carried out in Ref. [14] indicated the importance of microstructures in the local field distribution. In previous works, only the local field distribution was calculated. In this work, the response function of the model is obtained. With this function, one may determine all of the dielectric properties of the model. In principle, our treatment is not limited to the case of isotropic disorder and may be of use for more complex systems, perhaps even proteins. We turn to the details of our treatment now.

II. THEORETICAL FORMULATION

For a quenched disordered dielectric, we imagine that space is divided into a cubic grid of polarizable cells as pictured in Fig. 1(a). There exist three relevant length scales in this model. The first is a Gaussian length that is also the lattice spacing, a. It is the minimum length at which polarization field follows Gaussian statistics. In other words, in the volume specified by this Gaussian length a, the polarization is the result of a large enough number of molecular dipoles that this polarization will be close to a Gaussian random variable. The polarization of the cell $\mathbf{r}$ is $\mathbf{m}_\mathbf{r}$ with polarizability $\alpha_\mathbf{r}$. Specifically,

$$\alpha_\mathbf{r}=\beta\langle|\mathbf{m}_\mathbf{r}|^2\rangle_0, \tag{1}$$

where β is the usual inverse temperature, and $\langle\cdots\rangle_0$ denotes the thermal average over dipole fluctuations within a lattice cell for the idealized case where these dipoles do not interact with their surroundings. Interactions with surrounding dipoles renormalize this local polarizability in a fashion discussed below. In general, the polarizability of each cell is nonlocal in time in this reduced description, but we have restricted ourselves to the static case in this paper. The generalization to dynamical case can be done in a similar fashion as in Ref. [11].

The second length is a disorder length, which is the average distance over which there is a significant change in the polarizability defined over the Gaussian length. Figure 1(a) depicts a particular member of an ensemble of the model with a bimodal distribution of polarizabilities, the white lattice cell has a polarizable dipole with a lower polarizability, α_1, and the black cell has a polarizable dipole with a higher polarizability, α_2. In this case, the disorder length is given by the average distance between black cells or between white cells depending on which color of the cells has the lower concentration.

The third length is a solute length. It is the size of the probe molecule used in experimental measurements (not shown in the figure). This third length is relevant since it specifies the length scale resolved by experiments. We assume that this length is larger than the Gaussian length. An experimental length scale smaller than the Gaussian length would require a modification of the model we consider in this paper.

The Hamiltonian of the model can be written as

$$H=\frac{1}{2}\sum_{\mathbf{r}}^{N}\frac{\mathbf{m}_\mathbf{r}^2}{\alpha_\mathbf{r}}-\frac{1}{2}\sum_{\mathbf{r}\neq\mathbf{r}'}^{N}\mathbf{m}_\mathbf{r}\cdot\mathbf{T}_{\mathbf{r},\mathbf{r}'}\cdot\mathbf{m}_{\mathbf{r}'}. \tag{2}$$

$\mathbf{T}_{\mathbf{r},\mathbf{r}'}$ is the dipole-dipole interaction tensor for the system defined on the lattice with spacing a. In the limit that $a\rightarrow 0^+$, it becomes the familiar [8,10]

$$\mathbf{T}(\mathbf{r}-\mathbf{r}')=3\frac{(\mathbf{r}-\mathbf{r}')(\mathbf{r}-\mathbf{r}')}{|\mathbf{r}-\mathbf{r}'|^5}-\frac{\mathbf{I}}{|\mathbf{r}-\mathbf{r}'|^3}, \tag{3}$$

where $\mathbf{I}$ is the 3×3 identity matrix. In the discrete case, we use $\mathbf{T}_{\mathbf{r},\mathbf{r}'}=\mathbf{T}(\mathbf{r}-\mathbf{r}')$ for $\mathbf{r}\neq\mathbf{r}'$, and $\mathbf{T}_{\mathbf{r},\mathbf{r}}=\mathbf{0}$. The bimodal distribution for $\alpha_\mathbf{r}$ is assumed to be translationally invariant and spatially uncorrelated. Specifically

$$P(\alpha_\mathbf{r})=p_1\delta(\alpha_\mathbf{r}-\alpha_1)+(1-p_1)\delta(\alpha_\mathbf{r}-\alpha_2), \tag{4}$$

where a polarizable dipole with polarizability α_1 is located on a lattice site with a probability p_1. More complicated distributions are left to future analysis.

If the polarizability is a constant α over the whole material this model can be solved exactly [11]. For example, straightforward matrix mechanics demonstrates that the response function $\chi_{\mathbf{r},\mathbf{r}'}$ is given by

$$\chi_{\mathbf{r},\mathbf{r}'}=\frac{v\alpha}{1-y}\left[\frac{1+y}{1+2y}\delta_{\mathbf{r},\mathbf{r}'}\mathbf{I}+\frac{3y}{1+2y}\frac{v}{4\pi}\mathbf{T}_{\mathbf{r},\mathbf{r}'}\right], \tag{5}$$

where the dimensionless polarizability $y=4\pi\alpha\rho/3$, $\rho=1/v$, and $v=a^3$; $\delta_{\mathbf{r},\mathbf{r}'}$ is the Kronecker delta. In the continuum limit $a\rightarrow 0^+$, this result is the familiar dielectric continuum formula [9–11]

$$\chi(\mathbf{r}-\mathbf{r}')=\frac{\epsilon-1}{4\pi\rho\epsilon}\left[\frac{2\epsilon+1}{3}\delta(\mathbf{r}-\mathbf{r}')\mathbf{I}+\frac{\epsilon-1}{4\pi\rho}\mathbf{T}(\mathbf{r}-\mathbf{r}')\right], \tag{6}$$

where $\delta(\mathbf{r}-\mathbf{r}')$ is the Dirac delta function and ϵ is the dielectric constant related to the dimensionless polarizability y through the Clausius-Mossotti equation

$$\frac{\epsilon-1}{\epsilon+2}=y. \tag{7}$$

The renormalized local polarizability $\tilde{\alpha}$ is given by the full thermal average of the squared polarization fluctuations within a cell. With constant α, it is given by [11]

$$\tilde{\alpha}=\beta\langle|\mathbf{m}_\mathbf{r}|^2\rangle=\alpha\frac{(1+y)}{(1-y)(1+2y)}, \tag{8}$$

which is also the dielectric continuum result [9,11].

These connections between dielectric continuum formula and the bilinear Hamiltonian (2) lead one to identify the case with constant polarizability α as the dielectric continuum model. For applications concerned with solvation of microscopic entities, this terminology is somewhat a misnomer since the underlying Hamiltonian makes no physical sense unless the grid spacing a is finite and large enough that $\mathbf{m}_\mathbf{r}$ can obey Gaussian statistics.

In contrast to the case where $\alpha_\mathbf{r}$ is a constant, a spatially varying polarizability renders the diagonalization of the Hamiltonian very difficult if not impossible. To treat the model with a spatially random $\alpha_\mathbf{r}$, we develop a self-consistent theory of an inhomogeneous dielectric using the conventional dielectric continuum theory as a starting point. To this end, the whole material is divided into two parts. The first part, the primary system, is a finite lattice with the same polarizability distribution and the same lattice spacing as the original material. The second part, the secondary system, is the rest of the lattice with a constant polarizability $\bar{\alpha}$ to be determined self-consistently based on the material's polarizability distribution. This decomposition into primary and secondary systems is illustrated in Fig. 1(b). The overall dielectric response of the material is the net response of the combined primary and secondary subsystems. This treatment captures the inhomogeneity of the material and at the same time accounts for the long-range interactions in a dielectric material.

The Hamiltonian of the net system can be rewritten as

$$H=H_\mathrm{p}+H_\mathrm{b}+H_\mathrm{i}, \tag{9}$$

where

$$H_\mathrm{p}=\frac{1}{2}\sum_{\mathbf{r}\in\mathrm{p}}\frac{\mathbf{m}_\mathbf{r}^2}{\alpha_\mathbf{r}}-\frac{1}{2}\sum_{\mathbf{r}\neq\mathbf{r}'\in\mathrm{p}}\mathbf{m}_\mathbf{r}\cdot\mathbf{T}_{\mathbf{r},\mathbf{r}'}\cdot\mathbf{m}_{\mathbf{r}'}, \tag{10}$$

$$H_\mathrm{b}=\frac{1}{2}\sum_{\mathbf{r}\notin\mathrm{p}}\frac{\mathbf{m}_\mathbf{r}^2}{\bar{\alpha}}-\frac{1}{2}\sum_{\mathbf{r}\neq\mathbf{r}'\notin\mathrm{p}}\mathbf{m}_\mathbf{r}\cdot\mathbf{T}_{\mathbf{r},\mathbf{r}'}\cdot\mathbf{m}_{\mathbf{r}'}, \tag{11}$$

and

$$H_\mathrm{i}=-\sum_{\mathbf{r}\in\mathrm{p}}\sum_{\mathbf{r}'\notin\mathrm{p}}\mathbf{m}_\mathbf{r}\cdot\mathbf{T}_{\mathbf{r},\mathbf{r}'}\cdot\mathbf{m}_{\mathbf{r}'}. \tag{12}$$

Here, ''p'' stands for ''primary'' system, so that the sums over $\mathbf{r}\in\mathrm{p}$ are sums over lattice sites within the primary system. Similarly, sums over $\mathbf{r}\notin\mathrm{p}$ are sums over the lattice sites in the secondary system. H_i is the interaction between the primary system and the secondary system treated as an effective average medium (a dielectric continuum under the continuum limit), which is specified by $\bar{\alpha}$ and its lattice spacing a. The secondary subsystem plays a role of a ''bath'' linearly coupled to the primary system. For this reason, we use the subscript ''b'' to label the secondary system. Since the primary-secondary coupling involves long-ranged electrostatic interactions, the primary system feels an averaged effect of the secondary system. Therefore, provided a sensible criterion for choosing $\bar{\alpha}$ can be established, we expect the physical properties computed from this formulation should approach the exact properties of the system in the limit of a very large primary subsystem.

An effective Hamiltonian for the primary system can be defined by integrating out the degrees of freedom in the secondary system (bath degrees of freedom),

$$\exp[-\beta H_\mathrm{eff}]=\frac{\int_\mathrm{out}\mathcal{D}\mathbf{m}\exp(-\beta H_\mathrm{p}-\beta H_\mathrm{b}-\beta H_\mathrm{i})}{\int_\mathrm{out}\mathcal{D}\mathbf{m}\exp(-\beta H_\mathrm{b})}$$
$$=\exp(-\beta H_\mathrm{p})\langle\exp(-\beta H_\mathrm{i})\rangle_\mathrm{b}, \tag{13}$$

where $\int_\mathrm{out}\mathcal{D}\mathbf{m}$ denotes the integration over all $\mathbf{m}_\mathbf{r}$ for $\mathbf{r}$ not in the primary cell, i.e., $\mathbf{r}\notin\mathrm{p}$, and $\langle\cdots\rangle_\mathrm{b}$ means the thermal average over the bath variables. Since the bath polarization field is zero in the spatial region of the primary system, the statistics of this average is Gaussian, but with the constraint of no polarization in the primary system. The result of this constraint produces the bath response function $\chi^{(\mathrm{b})}_{\mathbf{r},\mathbf{r}'}$ [7,11]

$$\chi^{(\mathbf{b})}_{\mathbf{r},\mathbf{r}'}=\chi_{\mathbf{r},\mathbf{r}'}-\sum_{\mathbf{r}'',\mathbf{r}'''\in\mathrm{p}}\chi_{\mathbf{r},\mathbf{r}''}\cdot(\chi^{(\mathrm{p})})^{-1}_{\mathbf{r}'',\mathbf{r}'''}\cdot\chi_{\mathbf{r}''',\mathbf{r}'}. \tag{14}$$

Here, $\chi_{\mathbf{r},\mathbf{r}'}$ is given by Eq. (5) with $\alpha=\bar{\alpha}$; $(\chi^{(\mathrm{p})})^{-1}_{\mathbf{r},\mathbf{r}'}$ is nonzero only when both $\mathbf{r}$ and $\mathbf{r}'$ are within the primary region, and when this condition is met, it denotes the $\mathbf{r}\mathbf{r}'$ element of the matrix inverse of $\boldsymbol{\chi}^{(\mathrm{p})}$; the elements of this matrix, $\chi^{(\mathrm{p})}_{\mathbf{r},\mathbf{r}'}$, are nonzero only when both $\mathbf{r}$ and $\mathbf{r}'$ are within the primary region, and when this condition is met, the elements are given by $\chi_{\mathbf{r},\mathbf{r}'}$. With this notation, the result of integrating out the bath polarization field is

$$H_\mathrm{eff}=\frac{1}{2}\sum_{\mathbf{r}\in\mathrm{p}}\frac{\mathbf{m}_\mathbf{r}^2}{\alpha_\mathbf{r}}-\frac{1}{2}\sum_{\mathbf{r}\neq\mathbf{r}'\in\mathrm{p}}\mathbf{m}_\mathbf{r}\cdot\mathbf{T}_{\mathbf{r},\mathbf{r}'}\cdot\mathbf{m}_{\mathbf{r}'}$$
$$-\frac{1}{2}\sum_{\mathbf{r},\mathbf{r}'\in\mathrm{p}}\mathbf{m}_\mathbf{r}\cdot\left\{\sum_{\mathbf{r}'',\mathbf{r}'''}\mathbf{T}_{\mathbf{r},\mathbf{r}''}\cdot\chi^{(\mathrm{b})}_{\mathbf{r}'',\mathbf{r}'''}\cdot\mathbf{T}_{\mathbf{r}''',\mathbf{r}'}\right\}\cdot\mathbf{m}_{\mathbf{r}'}. \tag{15}$$

Substituting Eq. (14) into Eq. (15) and using the following identity:

$$\sum_{\mathbf{r}''}\mathbf{T}_{\mathbf{r},\mathbf{r}''}\cdot\mathbf{T}_{\mathbf{r}'',\mathbf{r}'}=\frac{4\pi}{3}\left[\frac{8\pi}{3}\delta_{\mathbf{r},\mathbf{r}'}\frac{\mathbf{I}}{v^2}-\frac{\mathbf{T}_{\mathbf{r},\mathbf{r}'}}{v}\right], \tag{16}$$

the final expression of our effective Hamiltonian is

$$H_\mathrm{eff}=\frac{1}{2}\sum_{\mathbf{r},\mathbf{r}'\in\mathrm{p}}\mathbf{m}_\mathbf{r}\cdot\mathbf{A}_{\mathbf{r},\mathbf{r}'}\cdot\mathbf{m}_{\mathbf{r}'}, \tag{17}$$

where

$$\mathbf{A}_{\mathbf{r},\mathbf{r}'}=\frac{1}{\alpha_{\mathbf{r}}}\delta_{\mathbf{r},\mathbf{r}'}\mathbf{I}-\mathbf{T}_{\mathbf{r},\mathbf{r}'}-\frac{3\bar{y}}{1+2\bar{y}}\left[\frac{8\pi}{9(1-\bar{y})}\delta_{\mathbf{r},\mathbf{r}'}\frac{\mathbf{I}}{v}+\frac{6\bar{y}-3}{9(1-\bar{y})}\mathbf{T}_{\mathbf{r},\mathbf{r}'}\right]+\sum_{\mathbf{r}'',\mathbf{r}'''\in \mathrm{p}}\frac{3\bar{y}}{4\pi(1+2\bar{y})}\mathbf{C}_{\mathbf{r},\mathbf{r}''}\cdot\mathbf{D}^{-1}_{\mathbf{r}'',\mathbf{r}'''}\cdot\mathbf{C}_{\mathbf{r}''',\mathbf{r}'}; \quad (18)$$

$$\mathbf{C}_{\mathbf{r},\mathbf{r}'}=\frac{8\pi\bar{y}}{3(1-\bar{y})}\delta_{\mathbf{r},\mathbf{r}'}\frac{\mathbf{I}}{v}+\frac{1}{1-\bar{y}}\mathbf{T}_{\mathbf{r},\mathbf{r}'}, \quad (19)$$

$$\mathbf{D}_{\mathbf{r},\mathbf{r}'}=\frac{1+\bar{y}}{1-\bar{y}}\delta_{\mathbf{r},\mathbf{r}'}\frac{\mathbf{I}}{v}+\frac{3\bar{y}}{4\pi(1-\bar{y})}\mathbf{T}_{\mathbf{r},\mathbf{r}'}. \quad (20)$$

In the next section, we establish a self-consistent criterion for identifying $\bar{y}=4\pi\rho\bar{\alpha}/3$. With this criterion, disorder is considered only as it appears explicitly in the primary system. A given realization of disorder in the primary system coincides with a given set of $\alpha_{\mathbf{r}}$ for all $\mathbf{r}\in \mathrm{p}$, chosen from its distribution [Eq. (4) being the specific example of the distribution considered herein]. We employ H_{eff} with a given realization of disorder in the primary system to compute a physical property associated with the primary system. This property can then be averaged over different realizations of the disorder to determine the predicted observed value for that property.

III. RENORMALIZATION TREATMENT OF THE EFFECTIVE HAMILTONIAN

A. Self-consistent evaluation of the dielectric response for the secondary system

To construct a self-consistent evaluation of $\bar{y}$, let us view the primary system as a single cell with lattice spacing na, where n^3 is the number of initial cells in the primary system. The total polarization of this new larger cell is

$$\mathbf{m}'=\sum_{\mathbf{r}\in \mathrm{p}}\mathbf{m}_{\mathbf{r}}. \quad (21)$$

Then, the renormalized polarizability associated with this new unit cell is

$$\tilde{\boldsymbol{\alpha}}'=\beta\langle\mathbf{m}'\mathbf{m}'\rangle_{\mathrm{eff}}=\beta\sum_{\mathbf{r}\in \mathrm{p}}\sum_{\mathbf{r}'\in \mathrm{p}}\langle\mathbf{m}_{\mathbf{r}}\mathbf{m}_{\mathbf{r}'}\rangle_{\mathrm{eff}}=\beta\sum_{\mathbf{r}\in \mathrm{p}}\sum_{\mathbf{r}'\in \mathrm{p}}\mathbf{A}^{-1}_{\mathbf{r},\mathbf{r}'}. \quad (22)$$

$\langle\cdots\rangle_{\mathrm{eff}}$ denotes the statistical average with Boltzmann weight $\exp(-\beta H_{\mathrm{eff}})$. The matrix $\mathbf{A}$, with elements given by Eq. (18), is determined by the polarizability of the secondary system and the particular realization of the disordered polarizabilities in the primary cells. That is to say, $\tilde{\boldsymbol{\alpha}}'=\tilde{\boldsymbol{\alpha}}'(\{\alpha_{\mathbf{r}},\mathbf{r}\in \mathrm{p}\},\bar{y})$. For a given realization of disorder in the primary system, $\tilde{\boldsymbol{\alpha}}'$ is generally a tensor. Due to the isotropic symmetry of the disorder distribution, however, $\tilde{\boldsymbol{\alpha}}'$ averaged over the different realization of the disorder is diagonal, with each of its diagonal elements equal.

The renormalization of the local polarizability is due to the coupling of the primary cell to the surrounding secondary system. Since we model the surroundings as an effective homogeneous secondary system with effective local polarizability $\bar{y}$, we can also obtain a renormalized polarizability $\tilde{\boldsymbol{\alpha}}'$ similar to Eq. (8), namely,

$$(\tilde{\boldsymbol{\alpha}}')^{-1}=(\boldsymbol{\alpha}')^{-1}-\mathbf{I}\frac{4\pi}{3(na)^3}\frac{2\bar{y}}{(1+\bar{y})}. \quad (23)$$

The above equation can be derived from Eqs. (17) and (22) if the primary system is viewed as a unit cell with lattice spacing na. Due to the homogeneity of the secondary system, this dimensionless polarizability $\bar{y}$ is invariant to the choice of grid spacing na, for $n=1,2,3\ldots$. That is, the dimensionless polarizability y is always defined as $4\pi\alpha/3(na)^3$. Equations (22) and (23) provide a formula for the unrenormalized local polarizability tensor,

$$(\boldsymbol{\alpha}')^{-1}=\left(\beta\sum_{\mathbf{r}\in \mathrm{p}}\sum_{\mathbf{r}'\in \mathrm{p}}\mathbf{A}^{-1}_{\mathbf{r},\mathbf{r}'}\right)^{-1}+\mathbf{I}\frac{4\pi}{3(na)^3}\frac{2\bar{y}}{(1+\bar{y})}, \quad (24)$$

which depends upon the set of $\alpha_{\mathbf{r}}$'s for $\mathbf{r}\in \mathrm{p}$ through the nonlinear dependence of $\mathbf{A}^{-1}_{\mathbf{r},\mathbf{r}'}$ on these variables. The distribution of $\boldsymbol{\alpha}'$ is of interest. For example, the distribution function for the dimensionless average diagonal component of $\boldsymbol{\alpha}'$ is

$$p(y';n,\bar{y})=\left\langle\delta\left[y'-\frac{4\pi}{3(na)^3}\mathrm{Tr}\,\boldsymbol{\alpha}'/3\right]\right\rangle_{\mathrm{av}}, \quad (25)$$

where Tr denotes the trace over Cartesian components of the tensor and a dimensionless polarizability y' is defined as $(4\pi/3(na)^3)\mathrm{Tr}\,\boldsymbol{\alpha}'/3$. $\boldsymbol{\alpha}'$ depends upon these $\alpha_{\mathbf{r}}$'s and $\bar{y}$ through Eq. (24), and $\langle\cdots\rangle_{\mathrm{av}}$ denotes the average over the realization of $\{\alpha_{\mathbf{r}}\}$ for $\mathbf{r}\in \mathrm{p}$,

$$\langle(\cdots)\rangle_{\mathrm{av}}=\int\prod_{\mathbf{r}\in \mathrm{p}}[d\alpha_{\mathbf{r}}P(\alpha_{\mathbf{r}})](\cdots). \quad (26)$$

A reasonable criterion for choosing $\bar{\alpha}$ and thus $\bar{y}$ is to have the average behavior of the primary cell coincide with that of the secondary system. In particular, the averaged renormalized polarizability is the same as the renormalized $\bar{y}$,

$$\frac{4\pi\beta}{9(na)^3}\left\langle\mathrm{Tr}\sum_{\mathbf{r}\in \mathrm{p}}\sum_{\mathbf{r}'\in \mathrm{p}}\mathbf{A}^{-1}_{\mathbf{r},\mathbf{r}'}\right\rangle_{\mathrm{av}}=\frac{\bar{y}(1+\bar{y})}{(1-\bar{y})(1+2\bar{y})}. \quad (27)$$

This association yields the self-consistent equation to be solved for $\bar{y}$. Iterations of these self-consistent equations converge fairly rapidly. For example, there is typically less than 1% drift in the value obtained for $\bar{y}$ after five or six iterations, where iterations are initiated by inserting $\bar{y}_0=(4\pi\rho/3)[p_1\alpha_1+(1-p_1)\alpha_2]$ as the value of $\bar{y}$ in the right-hand side of Eq. (22). The circles in Fig. 2 show the $\bar{y}$ from our self-consistent estimate for different values of p_1. It

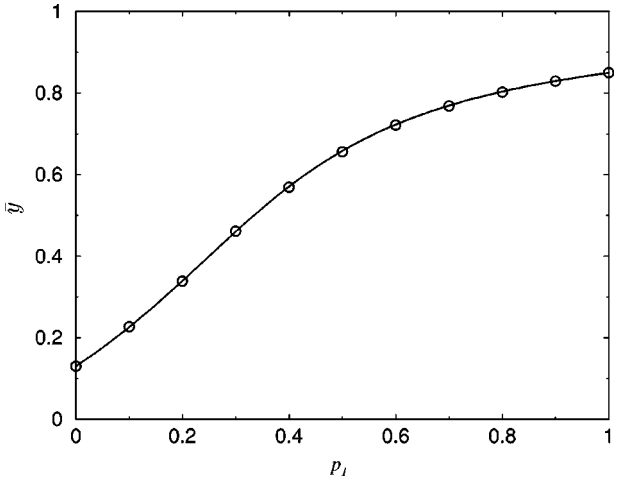

FIG. 2. The self-consistent polarizability as a function of polarizability distributions. The solid line is the effective medium theory, where $\bar{y}=\bar{y}_{\rm EM}$ is the physical root to Eq. (29). The circles are from our self-consistent calculation based on Eq. (27). The calculations are done for $y_1=0.85$, $y_2=0.13$. The primary system has 5^3 cells. The results are obtained by averaging 50 000 realizations.

should be noted that the conventional effective medium theory [15] is exactly recovered if the primary system only contains a single original unit cell. In this case, Eq. (27) becomes

$$p_1\left(\frac{1}{y_1}-\frac{2\bar{y}}{1+\bar{y}}\right)^{-1}+(1-p_1)\left(\frac{1}{y_2}-\frac{2\bar{y}}{1+\bar{y}}\right)^{-1}=\left(\frac{1}{\bar{y}}-\frac{2\bar{y}}{1+\bar{y}}\right)^{-1}, \tag{28}$$

where Eq. (23) has been used for the derivation and $y_i=(4\pi\rho/3)\alpha_i$ with $i=1$ or 2. Simple manipulations of Eq. (28) yield

$$p_1\frac{y_1-\bar{y}}{1+\bar{y}-2\bar{y}y_1}+(1-p_1)\frac{y_2-\bar{y}}{1+\bar{y}-2\bar{y}y_2}=0. \tag{29}$$

The physical root to Eq. (29) is identified by the requirement that $\bar{y}>0$. This solution, $\bar{y}_{\rm EM}$, coincides with an effective medium result [15]. The curve in Fig. 2 is generated from the effective medium theory and agrees with our self-consistent estimate. Thus, Eq. (27) can be viewed as a generalized effective medium result. A multiunit-cell primary system gives the same self-consistent $\bar{y}$ as the single unit-cell calculation. Therefore, the first moment of the distribution functions, $p(y';n,\bar{y})$, is well-described by the effective medium theory. Furthermore, our approach also gives the full distribution function of the polarizability. Typical distribution functions, $p(y';n,\bar{y})$, are illustrated in Fig. 3 for primary cells of a few different sizes. For primary cell lengths of $2a$ or $3a$, the local polarizability distribution is bimodal, reflecting the bimodal character of the under lying model. Once the primary system size is larger than 6^3 cells, however, the local polarizability distribution is unimodel and very nearly Gaussian. The small length where length scale renormalization cross-

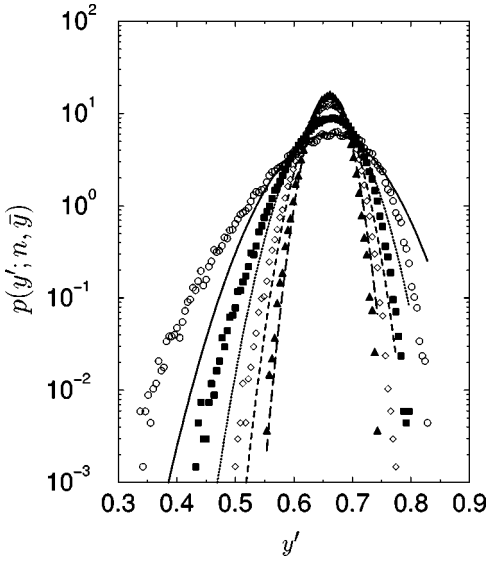

FIG. 3. The polarizability distribution as a function of primary system size. The symbols are from calculations based on Eq. (25) and the lines are fitting to a Gaussian distribution. The circles and the solid line are for 3^3 cells. The filled squares and the dotted line are for 4^3 cells. The diamonds and dashed line are for 5^3 cells. The filled triangles and the long-dashed line are for 6^3 cells. The calculations are done for $y_1=0.85$, $y_2=0.13$, and $p_1=0.5$.

over from bimodal to unimodel is nonuniversal, depending upon both system and property. For instance, the crossover length for local polarization field distributions [14] can be different than that for the local polarizability distribution.

The numerically determined distributions graphed in Fig. 3 were obtained by averaging over 50 000 realizations of the disordered primary system. Error estimates (not shown for clarity of the figure) gradually go from one fifth the size of the symbols in the peak region to about three times the size of the symbols in the wings of the distribution. This figure shows how the bimodal character of the basic cell distribution, $P(\alpha_{\mathbf{r}})$, becomes unimodal Gaussian-like with a width that decreases with increasing n. The size of primary cell

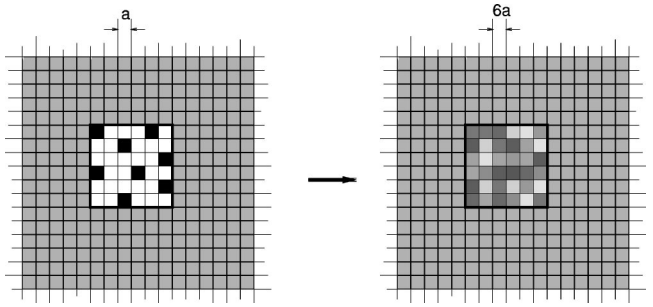

FIG. 4. An illustration of a renormalization flow in two dimensions. In the left panel, a particular realization of the primary system with bimodal distribution (black and white cells). As in Fig. 1, the gray cells in the secondary system represent the self-consistent dielectric continuum. In the right panel, each renormalized cell consists of 6^2 original cells in panel A. The new primary system has the same number (6^2) of new unit cells as the primary system in the left panel. The different gray levels of the cells denote a particular realization of the polarizability distribution calculated from the left panel.

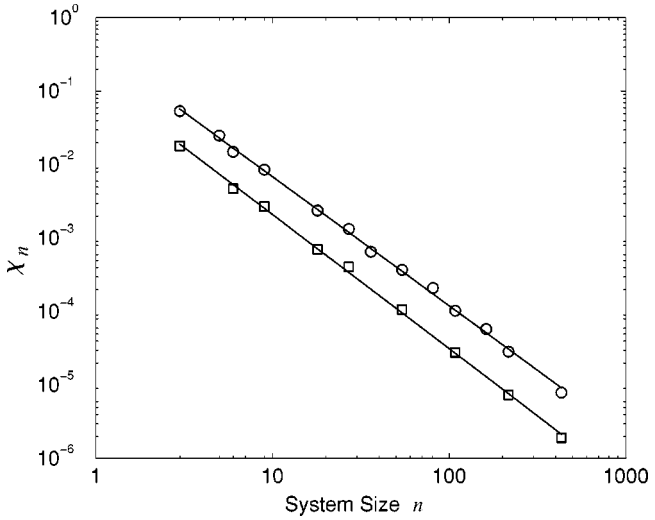

FIG. 5. The polarizability distribution width as a function of system size. The symbols are from calculations and the lines are power law fitting ($\chi_n \propto n^{\nu}$). Thus, the slope ν characterizes the decay of the distribution width. The spherical symbol set is for $p_1 = 0.5$ and the square symbol set for $p_1 = 0.8$. The same y_1 and y_2 are used as in Fig. 2.

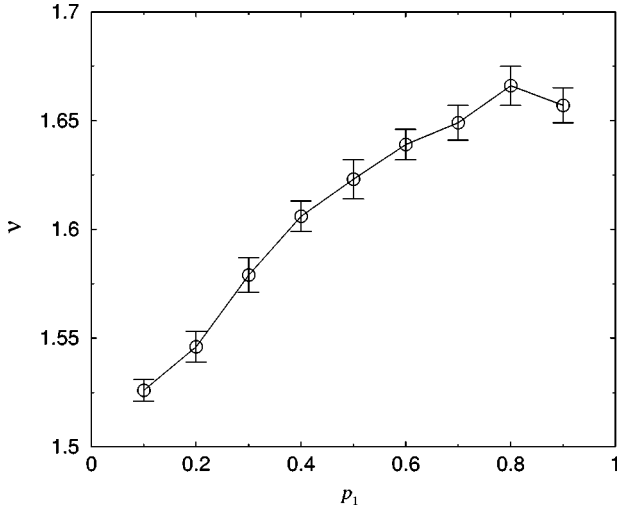

FIG. 6. The algebraically decay exponent as a function of p_1. The connecting line is a guide to the eye. The same y_1 and y_2 are used as in Fig. 2.

where the width of the polarizability distribution becomes negligible, indicates the length scale where the behavior of the model is that of a homogeneous dielectric with constant local polarizability $\overline{\alpha}$. In the next section, we focus on how this width or dispersion decreases with increasing length scale na.

B. The renormalization calculation of the effective polarizability distribution

When the primary system size is large, the matrix $\mathbf{A}_{\mathbf{r},\mathbf{r}'}$ is large, and it is computationally expensive to find the polarizability distribution directly. For example, if $n=7$, the calculation requires the inversion of a $(3\times 7)^3 = 9261$ by 9261 matrix for each realization of the ensemble. 50 000 realizations are needed to achieve a statistically satisfactory distribution. To circumvent this computational expense, we have devised a real space renormalization strategy. The strategy is based upon the observation that the polarizability distribution function $p(y';n,\overline{y})$ is essentially Gaussian when the length scale of the primary system na exceeds $4a$. The distribution of a larger primary system with length scale mna can be calculated by viewing it as a primary system with m^3 basic cells, where now the basic cell length is na. The local polarizability distribution for this basic cell of length scale na is $p(y'_{\mathbf{R}};n,\overline{y})$, where $\mathbf{R}$ refers to the position of a basic cell in the lattice with basic lattice spacing na. In this way, the self-consistent $\overline{y}$ and the distribution function $p(y';mn,\overline{y})$ is computed from Eqs. (25)–(23). In place of $P(y_{\mathbf{r}})$ in those earlier equations, one now uses $p(y'_{\mathbf{R}};n,\overline{y})$; in place of $\mathbf{r} \in \mathrm{p}$, one now uses $\mathbf{R} \in \mathrm{p}'$, where p' refers to the basic cells with length scale na that now form the primary cell with length scale mna; and in place of $p(y';n,\overline{y})$, one now obtains $p(y';mn,\overline{y})$.

This renormalization procedure is illustrated in Fig. 4. In three-dimension, the original primary system pictured on the left of Fig. 5 has 6^3 unit cells with lattice spacing a and the secondary system is an effective average medium with dimensionless polarizability $\overline{y}$ and lattice spacing a. After renormalization, pictured on the right side of the figure, the new lattice spacing is $6a$. The new primary system still has 6^3 basic cells, as before, but these new basic cells have a basic length six times larger than before. Further, the disorder distribution for the new basic renormalized cell is the distribution of the primary system before renormalization. In

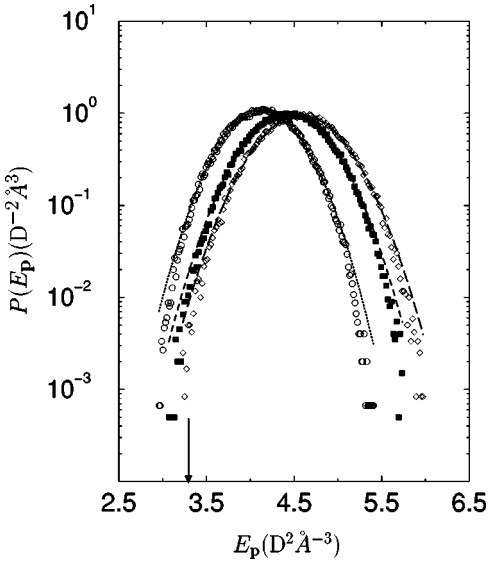

FIG. 7. The solvation energy distribution of a dipole in a random dielectric material. As the size of our primary system increases, the probability distribution converges to a Gaussian distribution. The arrow indicates the value of $E_{\mathbf{p}}(\overline{y}_{\mathrm{EM}})$, where $\overline{y}_{\mathrm{EM}}$ is the effective medium approximation given by the positive root of Eq. (29). The symbols are from calculations based on Eq. (34) and the lines are a Gaussian distribution fitting. The circles and the dotted line are for solute size $n=4$. The filled square and the dashed line are for $n=6$. The diamonds and the long-dashed line are for $n=8$. The same y_1 and y_2 are used as in Fig. 2 and $p_1=0.5$. The size of the dipole is 1.0 D.

addition to the effective medium reaction field approximation that is inherent to our approach, this renormalization procedure introduces an additional approximation. In particular, the renormalization approach neglects correlations in disorder between different renormalized basic cells. While the initial model has no such correlations between different original unit cells, by construction, the statistics of $y'_{\mathbf{R}}$ is correlated to $y'_{\mathbf{R}'}$ for $\mathbf{R}\neq\mathbf{R}'$.

Applying this renormalization method, one may estimate the results of calculations for primary systems of essentially arbitrary length scale. As the length scale increases, the width of the polarizability distribution decreases. The variation of this width, χ_n, with changing length scale na, is illustrated in Fig. 5. It is defined as

$$\chi_n^2=\int dy'(\delta y')^2 p(y';mn,\bar{y}), \tag{30}$$

where $\delta y'$ denotes the deviation of y' from its average, i.e., the first moment of $p(y';mn,\bar{y})$. We see that χ_n decays algebraically as a function of the primary system size. By fitting the distribution width as a function of the primary system size n with the function form $\chi_n\propto n^{\nu}$, the decay exponent ν is obtained. Figure 5 shows the decay exponents extracted in this way for primary cells with lengths of the order of 10^2a. The exponents vary weakly as a function of probability p_1, remaining close in value to $\nu\approx 2.0$. A renormalization group calculation [16] predicts that $\nu=2.0$ is the universal decay exponent in the continuum limit. The weak dependence upon p_1 illustrated in Fig. 6 shows that the continuum limit is not yet reached for the primary cells with lengths of the order of 10^2a. The fact that χ_n decays as a power of n indicates that there does not exist a correlation length for such inhomogeneous dielectrics. The existence of a correlation length would imply that the width of the distribution would decay exponentially as a function of primary system size.

IV. SOLVATION ENERGY OF A DIPOLE IN A RANDOM DIELECTRIC MATERIAL

We now turn to the issue of estimating solvation energy statistics. We consider explicitly solvation energies for dipoles in the disordered system. Similar results will follow for reorganization energies, as noted below. For a given realization of disorder, these quantities have specific values. The distribution of disorder, however, results in distributions of values. One experimental consequence of the distributions concerns kinetics of electron transfer. According to Marcus's theory [17], the rate constant for an electron transfer reaction k_{ET} is given by the energy gap law, $k_{\mathrm{ET}}\sim\exp[-\beta(\lambda+\Delta G)^2/4\lambda]$. Here, λ is the reorganization energy and ΔG is the thermodynamic driving force. In part, ΔG is the difference between the reactant and product solvation energies. To the extent that these quantities are statistically distributed rather than constant, the observed survival probability for the reactant redox state must be computed by averaging $\exp(-k_{\mathrm{ET}}t)$ over the distributions for λ and ΔG. Such inhomogeneous averaging has been used to interpret the nonexponential kinetics observed in the primary electron transfer of photosynthesis [18]. Thus, a theory for the distributions of λ and ΔG can be relevant to experiments.

To estimate these distributions, we consider a dipole $\mathbf{p}$ in a cell at origin, $\mathbf{r}=\mathbf{0}$, a primary system with length scale na surrounding the origin, and an effective medium with constant local polarizability $\bar{\alpha}$ surrounding the primary cell. For a particular realization of the random polarizabilities in the primary system cell, the effective Hamiltonian is

$$\begin{aligned}H_{\mathbf{p}}=&\frac{1}{2}\sum_{\mathbf{r},\mathbf{r}'\in\mathrm{p}}\mathbf{m}_{\mathbf{r}}\cdot\mathbf{A}_{\mathbf{r},\mathbf{r}'}\cdot\mathbf{m}_{\mathbf{r}'}-\mathbf{p}\cdot\sum_{\mathbf{r}\in\mathrm{p}}\left\{\frac{1}{(1-\bar{y})(1+2\bar{y})}\mathbf{T}_{\mathbf{0},\mathbf{r}}\right.\\&\left.-\frac{3\bar{y}}{4\pi(1+2\bar{y})}\sum_{\mathbf{r}',\mathbf{r}''\in\mathrm{p}}\mathbf{C}_{\mathbf{0},\mathbf{r}'}\cdot\mathbf{D}^{-1}_{\mathbf{r}',\mathbf{r}''}\cdot\mathbf{C}_{\mathbf{r}'',\mathbf{r}}\right\}\cdot\mathbf{m}_{\mathbf{r}}\\&-\frac{1}{2}\mathbf{p}\cdot\left\{\frac{8\pi\bar{y}}{3v(1-\bar{y})(1+2\bar{y})}\mathbf{I}\right.\\&\left.-\frac{3\bar{y}}{4\pi(1+2\bar{y})}\sum_{\mathbf{r}',\mathbf{r}''\in\mathrm{p}}\mathbf{C}_{\mathbf{0},\mathbf{r}'}\cdot\mathbf{D}^{-1}_{\mathbf{r}',\mathbf{r}''}\cdot\mathbf{C}_{\mathbf{r}'',\mathbf{r}}\right\}\cdot\mathbf{p},\end{aligned}\tag{31}$$

where $\bar{y}$ has been obtained self-consistently in the absence of the dipole from Eq. (23). The first term sums the effective medium averaged interactions between all dipoles in the primary system excepting the solute dipole at the origin. The second term adds the effective medium averaged interactions between the solute dipole and the other polarizable dipoles in the primary system. The third term is the effective medium averaged self-energy reaction of the solute dipole. The solvation energy of the dipole, $E_{\mathbf{p}}$, is given by the usual ratio of partition functions with and without the solute,

$$\exp(-\beta E_{\mathbf{p}})=\frac{\int_{\mathrm{in}}\mathcal{D}\mathbf{m}_{\mathbf{r}}\exp(-\beta H_{\mathbf{p}})}{\int_{\mathrm{in}}\mathcal{D}\mathbf{m}_{\mathbf{r}}\exp(-\beta H_{\mathbf{0}})},\tag{32}$$

where $H_{\mathbf{0}}$ is the first term in Eq. (31), and $\int_{\mathrm{in}}\mathcal{D}\mathbf{m}_{\mathbf{r}}$ denotes the integration over $\mathbf{m}_{\mathbf{r}}$ for $\mathbf{r}\in\mathrm{p}$, excepting $\mathbf{r}=\mathbf{0}$. Evaluation of the Gaussian integrals yields the solvation energy $E_{\mathbf{p}}$,

$$\begin{aligned}E_{\mathbf{p}}=&-\frac{1}{2}\mathbf{p}\cdot\sum_{\mathbf{r},\mathbf{r}'''\in\mathrm{p}}\left\{\frac{1}{(1-\bar{y})(1+2\bar{y})}\mathbf{T}_{\mathbf{0},\mathbf{r}}\right.\\&\left.-\frac{3\bar{y}}{4\pi(1+2\bar{y})}\sum_{\mathbf{r}',\mathbf{r}''\in\mathrm{p}}\mathbf{C}_{\mathbf{0},\mathbf{r}'}\cdot\mathbf{D}^{-1}_{\mathbf{r}',\mathbf{r}''}\cdot\mathbf{C}_{\mathbf{r}'',r}\right\}\\&\times(\mathbf{A}^{-1})_{\mathbf{r},\mathbf{r}'''}\cdot\left\{\frac{1}{(1-\bar{y})(1+2\bar{y})}\mathbf{T}_{\mathbf{r}''',\mathbf{0}}\right.\\&\left.-\frac{3\bar{y}}{4\pi(1+2\bar{y})}\sum_{\mathbf{r}',\mathbf{r}''\in\mathrm{p}}\mathbf{C}_{\mathbf{r}''',\mathbf{r}'}\cdot\mathbf{D}^{-1}_{\mathbf{r}',\mathbf{r}''}\cdot\mathbf{C}_{\mathbf{r}'',\mathbf{0}}\right\}\cdot\mathbf{p}\\&-\frac{1}{2}\mathbf{p}\cdot\left\{\frac{8\pi\bar{y}}{3v(1-\bar{y})(1+2\bar{y})}\mathbf{I}\right.\\&\left.-\frac{3\bar{y}}{4\pi(1+2\bar{y})}\sum_{\mathbf{r}',\mathbf{r}''\in\mathrm{p}}\mathbf{C}_{\mathbf{0},\mathbf{r}'}\cdot\mathbf{D}^{-1}_{\mathbf{r}',\mathbf{r}''}\cdot\mathbf{C}_{\mathbf{r}'',\mathbf{r}}\right\}\cdot\mathbf{p}.\end{aligned}\tag{33}$$

Similar expressions can be derived for reorganization energies. In this case, however, the expressions involve differ-

ences between solvation energies at low dielectric response frequency and solvation [17,19]. The former are given by expressions such as Eq. (33), involving the random local zero frequency polarizability. The latter are also given by such expressions, but involving the local high frequency electronic polarizability. This high frequency polarizability will have a far smaller dispersion than the zero frequency polarizability. To a reasonable approximation, therefore, the dispersion of reorganization energy is about the same size as the dispersion of solvation energy.

With Eq. (33), the distribution function for $E_{\mathbf{p}}$ is estimated as

$$P(E_{\mathbf{p}}) = \langle \delta[E_{\mathbf{p}} - E_{\mathbf{p}}(\{\alpha_{\mathbf{r}}, \mathbf{r} \in \mathrm{p}\}, \bar{y})] \rangle_{\mathrm{av}} = \int \prod_{\mathbf{r} \in \mathrm{p}, \mathbf{r} \neq \mathbf{0}} [d\alpha_{\mathbf{r}} P(\alpha_{\mathbf{r}})] \delta[E_{\mathbf{p}} - E_{\mathbf{p}}(\{\alpha_{\mathbf{r}}, \mathbf{r} \in \mathrm{p}\}, \bar{y})]. \tag{34}$$

Figure 7 illustrates this distribution computed for a few different primary system sizes for the case where $p_1 = 0.5$ and $\mathbf{p} = 1.0$ D. The results are obtained by 50 000 realizations. Error estimates (not shown for clarity of the figure) gradually go from one-fifth the size of the symbols in the peak region to about three times the size of the symbols in the wings of the distribution. In the limit of a very large primary system, the distribution will tend to the exact one for this model. Judging from the relative changes in going from $n = 4$ to 6 to 8, it appears that $n = 8$ is close to the infinite system limit. The δ-function distribution, indicated by a vertical line with an arrow in Fig. 7, represents a dielectric continuum limit of the model. In this dielectric continuum limit, the outside dielectric medium is represented by a dielectric continuum whose dielectric $\bar{y}$ is given by our self-consistent calculation. From Eq. (33), the solvation energy $E_{\mathbf{p}}$ can be obtained by setting $\mathbf{r} = \mathbf{0}$ and $\mathbf{r}''' = \mathbf{0}$. This dielectric continuum prediction gives $E_{\mathbf{p}} = 3.29$ D^{2}Å^{-3} without dispersion. In contrast, the mean $\langle E_{\mathbf{p}} \rangle$, and root mean-square dispersion $\langle (\delta E_{\mathbf{p}})^2 \rangle^{1/2}$ predicted from the $n = 8$ distribution are 4.58 D^{2}Å^{-3} and 0.39 D^{2}Å^{-3}, respectively. Thus, inhomogeneity of a dielectric material can indeed significantly affect solvation and reorganization energies.

ACKNOWLEDGMENTS

X.S. (the initial part of this work at Berkeley) and D.C. are grateful for the financial support from the Office of Basic Energy Sciences, Chemical Sciences Division of the U.S. Department of Energy under Contract No. DE-FG03-87ER13793.

[1] For example, M. Maroncelli and G.R. Fleming, J. Chem. Phys. **89**, 5044 (1988).
[2] J.S. Bader and D. Chandler, Chem. Phys. Lett. **157**, 501 (1989).
[3] B. Bagchi, D.W. Oxtoby, and G.R. Fleming, Chem. Phys. **86**, 257 (1984).
[4] C.P. Hsu, X. Song, and R.A. Marcus, J. Phys. Chem. **101**, 2546 (1997).
[5] X. Song and D. Chandler, J. Chem. Phys. **108**, 2594 (1998).
[6] M.J. Lang, X.J. Jordanides, X. Song, and G.R. Fleming, J. Chem. Phys. **110**, 5884 (1999).
[7] D. Chandler, Phys. Rev. E **48**, 2898 (1993).
[8] J.D. Jackson, *Classical Electrodynamics*, 2nd ed. (Wiley, New York, 1975).
[9] C.J.F. Böttcher and P. Bordewijk, *Theory of Electric Polarizations* (Elsevier, Amsterdam, 1973), Vol. 1.
[10] M.S. Wertheim, Annu. Rev. Phys. Chem. **30**, 471 (1979).
[11] X. Song, D. Chandler, and R.A. Marcus, J. Phys. Chem. **100**, 11 954 (1996).
[12] R.R. Netz and A.N. Berker, Phys. Rev. Lett. **66**, 377 (1991); A. Falicov, A.N. Berker, and S.R. McKay, Phys. Rev. B **51**, 8266 (1995), and references therein.
[13] M. Barthélémy and H. Orland, Phys. Rev. D **56**, 2835 (1997).
[14] Z. Chen and P. Sheng, Phys. Rev. B **43**, 5735 (1991).
[15] R. Landauer, in *Electrical Transport and Optical Properties of Inhomogeneous Media*, edited by J.C. Garland and D.B. Tanner (AIP, New York, 1978); A. Gonis, *Green Functions for Ordered and Disordered Systems* (Elsevier, North-Holland, Amsterdam, 1993).
[16] Z.G. Yu, X. Song, and D. Chandler, Phys. Rev. E **62**, 4698 (2000).
[17] R.A. Marcus, Rev. Mod. Phys. **65**, 599 (1993).
[18] For example, Z. Wang, R.M. Pearlstein, Y. Jia, and G.R. Fleming, Chem. Phys. **176**, 421 (1993).
[19] D. Chandler, in *Computer Simulation of Rare Events and Dynamics of Classical and Quantum Condensed-Phase Systems—Classical and Quantum Dynamics in Condensed Phase Simulations*, edited by B.J. Berne, G. Ciccotti, and D.F. Coker (World Scientific, Singapore, 1998), pp. 25–49.